

# Signal quality in digitally modulated scaled laser diodes

S. M. K. Thiyagarajan and A. F. J. Levi  
Department of Electrical Engineering  
University of Southern California, Los Angeles  
California 90089-1111

## Abstract

The calculated behavior of Gb/s on-off modulated scaled microlasers exhibit a non-monotonic dependence of timing jitter on spontaneous emission factor,  $\beta$ . Microlasers with  $10^{-2} < \beta < 10^{-1}$  give optimal performance for Gb/s on-off modulated applications requiring less than 20 ps jitter and greater than 20 dB optical power contrast ratio.

## 1. Introduction

Advances in microlaser processing will result in devices with ultra-low threshold current and photon cavity volumes approaching a cubic wavelength. In such microlasers the spontaneous emission factor,  $\beta$  may be tailored to meet the needs of a given application. In this paper we analyze microlaser output signal quality as a function of  $\beta$ . Signal quality is parametrized in terms of timing jitter,  $\sigma$  average turn-on delay,  $t_d$  and optical output power contrast ratio, C for below to above laser threshold current (on-off) modulation at 1 Gb/s and in terms of  $\sigma$  and  $t_d$  for on-on modulation at 1 Gb/s.

## 2. Model and simulation

Rate equations with Langevin noise source terms [1] are used to estimate  $t_d$  and  $\sigma$  for a scaled laser diode.

$$\frac{dS}{dt} = (G - \kappa)S + \beta R_{sp} + F_{si}(t) \quad (1)$$

and

$$\frac{dN}{dt} = \left(\frac{I}{e}\right) - GS - \frac{N}{\tau_n} + F_{ei}(t) \quad (2)$$

where S and N are total photon and carrier (electron) numbers in the cavity, G ( $\kappa$ ) is the optical gain (loss),  $\beta$  is the fraction of the total spontaneous emission that couples into the lasing mode. Variation in  $\beta$  may arise from a change in photon cavity volume and / or from quantum electrodynamic (QED) effects.  $R_{sp}$  is the spontaneous emission into all optical modes and  $F_{si}$ ,  $F_{ei}$  are Langevin noise terms [1, 2].  $F_{si}$  and  $F_{ei}$  are Gaussian random variables, which in the Markovian approximation have autocorrelation functions,

$$\langle F_{si}(t)F_{si}(t') \rangle = ((G + \kappa)S + \beta R_{sp})\delta(t - t') \quad (3)$$

$$\langle F_{ei}(t)F_{ei}(t') \rangle = (I/e + GS + N/\tau_n)\delta(t - t') \quad (4)$$

We assume no crosscorrelation between the noise terms and the non-Markovian contribution to noise for times shorter than the  $\sim 100$  fs electron scattering rate is set to zero.

Inset to Figure 1(a) illustrates  $t_d$  and  $\sigma$  in laser output relative to deterministic Non-Return-to-

Zero (NRZ) current modulation applied to the laser diode between  $I_{\text{low}}$  and  $I_{\text{high}}$ . For on-off modulation  $I_{\text{low}} < I_{\text{th}} < I_{\text{high}}$  where  $I_{\text{th}}$  is the laser threshold current. For on-on modulation  $I_{\text{th}} < I_{\text{low}} < I_{\text{high}}$ .  $S_{\text{low}}$  ( $S_{\text{high}}$ ) is the average steady-state number of cavity photons corresponding to an injection current of  $I_{\text{low}}$  ( $I_{\text{high}}$ ).  $t_d$  is the average time to reach a total number of cavity photons which is 50% of the difference in steady-state values such that  $S(t = t_d) = (S_{\text{high}} + S_{\text{low}})/2$ . The random nature of spontaneous emission gives rise to a distribution in turn-on delay with standard deviation  $\sigma$ . We assume lasing in a single longitudinal mode, linear optical gain  $G = \Gamma g_{\text{slope}} v_g (N/V - n_0)$  with  $g_{\text{slope}} = 4.8 \times 10^{-16} \text{ cm}^2$ , optical transparency carrier density  $n_0 = 1.5 \times 10^{18} \text{ cm}^{-3}$ , optical mode confinement factor  $\Gamma = 0.1$ , photon group velocity  $v_g = 8.1 \times 10^9 \text{ cm s}^{-1}$ , and active volume  $V = 2 \times 10^{-13} \text{ cm}^3$ . The  $10 \text{ cm}^{-1}$  internal loss and radiative recombination coefficient  $B = 1 \times 10^{-10} \text{ cm}^3 \text{ s}^{-1}$  used in our study are typical of InGaAsP lasers [3]. Ignoring QED effects,  $R_{\text{sp}} = BN^2/V = N/\tau_n$  is assumed.

### 3. Results

Shown in Figure 1(a) is the dependence of  $t_d$  and  $\sigma$  as a function of  $\beta$  for an ultra-low threshold current on-off modulated  $1 \mu\text{m}$  long microlaser photon cavity with 99% mirror reflectivity. The threshold current is  $I_{\text{th}} = 46 \mu\text{A}$  and the electrical input to the laser is modulated between  $I_{\text{low}} = 8 \mu\text{A}$  and  $I_{\text{high}} = 138 \mu\text{A}$ . The continuous decrease in  $t_d$  with increasing  $\beta$  shown in Figure 1(a) is due to the accompanying increase in  $S_{\text{low}}$ . Spontaneous emission is the dominant recombination process below threshold so an increase in  $\beta$  increases  $S_{\text{low}}$ . Figure 1(a) also shows that timing jitter does not vary monotonically with  $\beta$ . This non-monotonic dependence of jitter on  $\beta$  is due to two competing effects: (i) Enhancement in spontaneous emission noise with increase in  $\beta$  increases  $\sigma$ . (ii) The time for which spontaneous emission influences jitter depends on  $t_d$  so an increase in  $\beta$  which decreases  $t_d$  reduces  $\sigma$ . As shown in Figure 1(a), effects (i) and (ii) compensate each other so that values of  $\beta > 10^{-2}$  do not yield further reduction in  $\sigma$ .

Signal power contrast ratio is  $C = S_{\text{high}}/S_{\text{low}}$ . A larger value of  $C$  indicates better signal quality. As shown in Figure 1(b), for a fixed  $I_{\text{high}}$  and  $I_{\text{low}}$ ,  $C$  decreases continuously with an increase in  $\beta$ .

When the laser is biased below threshold, spontaneous emission dominates and the total number of cavity photons contributing to  $S_{\text{low}}$  is strongly dependent on  $\beta$ . Hence,  $S_{\text{low}}$  increases significantly with an increase in  $\beta$ . Well above threshold, stimulated emission dominates and hence  $S_{\text{high}}$  shows a very weak dependence on  $\beta$  leading to a small increase in  $S_{\text{high}}$  with increase in  $\beta$ . To overcome this degradation in  $C$  with increase in  $\beta$ , one may increase  $I_{\text{high}}$  which leads to greater power consumption. Alternately, one may decrease  $I_{\text{low}}$  which leads to larger  $t_d$  and increased electronic delay due to the larger voltage swing across the laser diode that occurs for a given current swing. The latter effect is due to the exponential dependence of the laser diode's current on the voltage across it. Low-cost systems with Gb/s on-off modulation which simultaneously require  $C > 20$  dB and  $\sigma < 20$  ps will benefit from use of micro-lasers with  $10^{-2} < \beta < 10^{-1}$ . At present, this is attractive because technologically it is easier to make microlasers with spontaneous emission coupling into  $\sim 100$  modes than microlasers with spontaneous emission coupling into less than 5 modes.

Figure 2 shows the effect of varying  $\beta$  when the device is on-on (above threshold) modulated between  $I_{\text{low}} = 100 \mu\text{A}$  and  $I_{\text{high}} = 400 \mu\text{A}$ . The turn-on delay increases with an increase in  $\beta$ . This can be understood as follows:  $t_d$  of an on-on modulated laser with  $\beta \sim 0$  is limited by the ps stimulated emission time while  $t_d$  of a laser with  $\beta \sim 1$  is affected by the ns carrier lifetime. Hence,  $t_d$  increases as  $\beta$  increases. Jitter is insensitive to  $t_d$  and is found to be approximately 5 - 6 ps for all values of  $\beta$ . Errors due to the finite number of samples used in our calculations mask subtle variations of  $\sigma$  with  $\beta$  and  $t_d$ .

Figure 2 shows that for high-speed ( $> 10$  Gb/s), low-contrast (on-on modulation) systems which are limited by turn-on delay, it is not advantageous to use microlasers with  $\beta$  close to unity. Further, one can see that values of  $10^{-2} < \beta < 10^{-1}$  lead to comparatively low turn-on  $\sigma$  and  $t_d$  both for on-on and on-off modulation. For on-on modulation one expects negligible dependence of contrast ratio on  $\beta$ .

#### 4. Discussion

In this work, we assume cavity QED effects that occur in micro-lasers do not alter  $R_{sp}$  although it has been shown that by suitably designing the cavity  $R_{sp}$  can be enhanced or suppressed [4]. Nevertheless, the trends discussed in this work remain valid even for arbitrary changes to  $\beta$  for a given  $R_{sp}$ . Another assumption is that gain experienced by a mode is independent of  $\beta$ . In fact, equilibrium modal gain should be linearly dependent on the spontaneous emission coupling into the mode. An enhancement of  $g_{slope}$  with an increase in  $\beta$  leads to lower  $I_{th}$  and hence, for fixed values of  $I_{low}$  and  $I_{high}$ , a degradation in  $C$  for on-off modulation. This is because, in the limit of  $I_{th}$  going below  $I_{low}$ , the contrast ratio reduces to that of on-on modulation. The increase in  $g_{slope}$  which accompanies an increase in  $\beta$  will tend to decrease even further the turn-on delays at higher  $\beta$ . Hence, the trends seen from Figures 1(a) and 1(b) will only be enhanced if  $g_{slope}$  were to increase with an increase in  $\beta$ . The results of our study for on-off modulation remain valid if the modal gain depends on spontaneous emission coupling into that mode. However, for on-on modulation an enhancement in  $g_{slope}$  with an increase in  $\beta$  improves the high-speed response and reduces the turn-on delay. To study this dependence a self-consistent dynamic model which describes the interplay of  $\beta$ ,  $R_{sp}$ , and  $G$  in a microcavity is required.

#### 5. Conclusion

In conclusion,  $\sigma$  for an on-off modulated laser varies with  $\beta$  in a non-monotonic fashion, while  $t_d$  decreases monotonically. Microlasers with  $10^{-2} < \beta < 10^{-1}$  give optimum performance for modest bit rate ( $\sim 1$  Gb/s),  $\sigma < 20$  ps,  $C > 20$  dB on-off modulation and comparatively low values of  $t_d$  ( $\sim 40$  ps) for on-on modulation.

#### Acknowledgment:

This work is supported in part by the Joint Services Electronics Program under contract #F49620-94-0022, and DARPA Ultra-II / Air Force Office of Scientific Research under contract #F49620-97-1-0438.

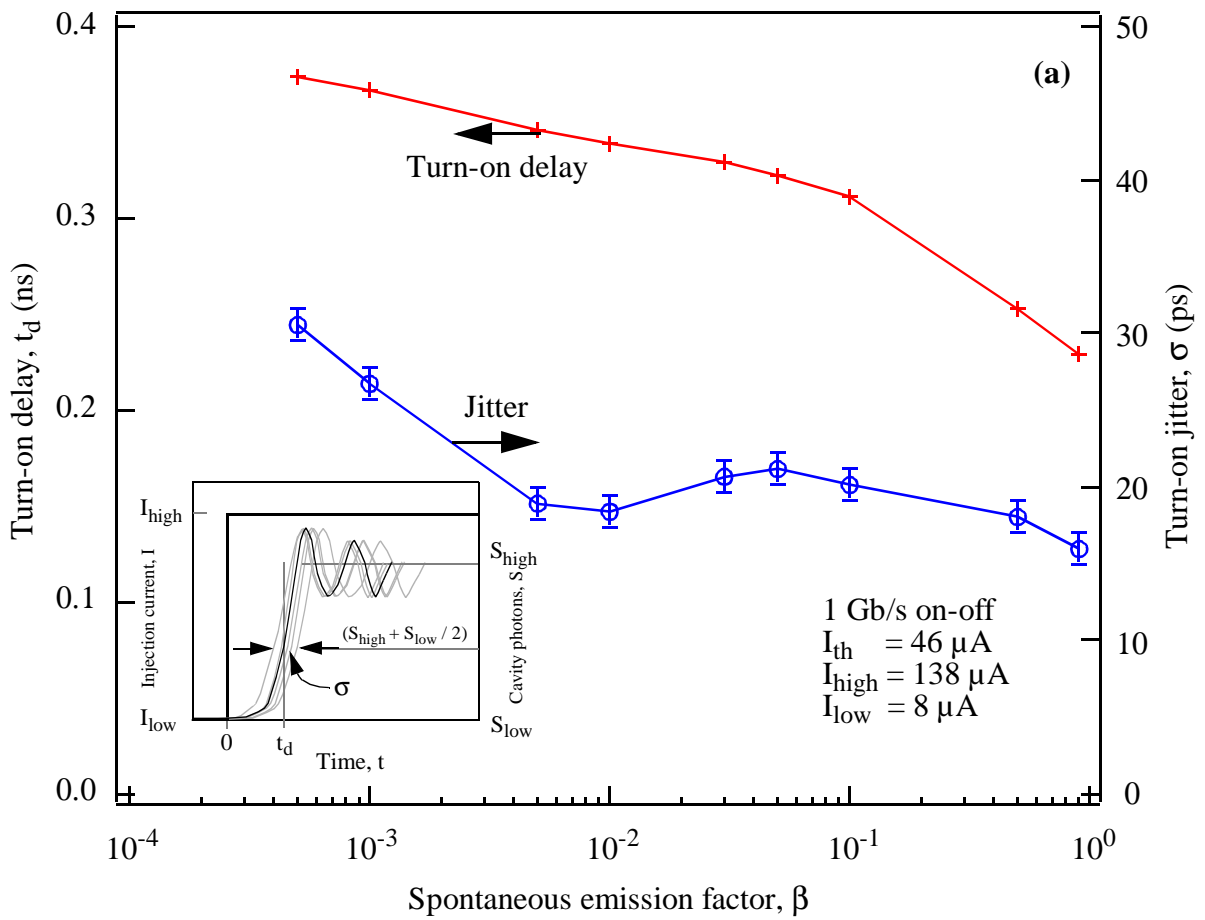
## References:

- [1] Marcuse, D., *IEEE J. of Quantum Electron.* **QE-20**, 1984, 1139 and 1148.
- [2] Schell, M., Huhse, D., Utz, W., Kaessner, J., Bimberg, D., and Tarasov, I. S., *IEEE J. Selected topics in Quantum Electron.* **1**, 1995, 528.
- [3] Agrawal, G. P., and Dutta, N. K., *Semiconductor Lasers*, 2nd Ed., p. 238, Van Nostrand Reinhold, New York, New York, 1993.
- [4] Bjork, G., and Yamamoto, Y., *IEEE J. of Quantum Electron.* **QE-27**, 1991, 2386.

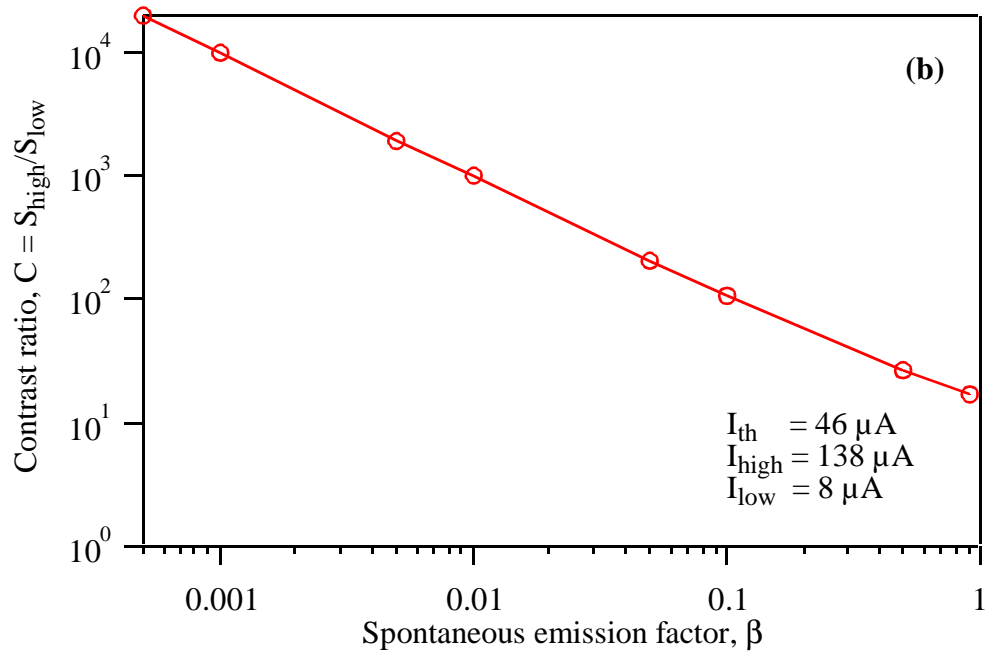
## Figure Captions.

Figure 1: (a) Calculated effect of  $\beta$  on  $t_d$  and  $\sigma$  for 1010 .... NRZ 1 Gb/s on-off modulation with  $I_{\text{high}} = 138 \mu\text{A}$  and  $I_{\text{low}} = 8 \mu\text{A}$ . Cavity length is  $1 \mu\text{m}$  and volume of the microlaser active region is  $2 \times 10^{-13} \text{ cm}^3$ . The mirror reflectivity is 99% leading to a threshold current of  $I_{\text{th}} = 46 \mu\text{A}$ . Error bars are due to finite number ( $\sim 800$ ) of samples and the pseudo-random number generator used to calculate jitter. Inset is illustration of electrical signal applied to laser diode versus time and the number of cavity photons, indicating  $t_d$  and  $\sigma$ . (b) Calculated log - log plot of  $C = S_{\text{high}}/S_{\text{low}}$  versus  $\beta$  for the device simulated in Figure 1(a). A continuous degradation in contrast ratio with an increase in  $\beta$  is seen. The circles represent the data obtained using our simulations. The line is to guide the eye.

Figure 2: Calculated effect of  $\beta$  on  $t_d$  and  $\sigma$  for 1010 .... NRZ 1 Gb/s on-on modulation with  $I_{\text{high}} = 400 \mu\text{A}$  and  $I_{\text{low}} = 100 \mu\text{A}$  for the microlaser corresponding to Figure 1.



**Figure 1(a)**



**Figure 1(b)**

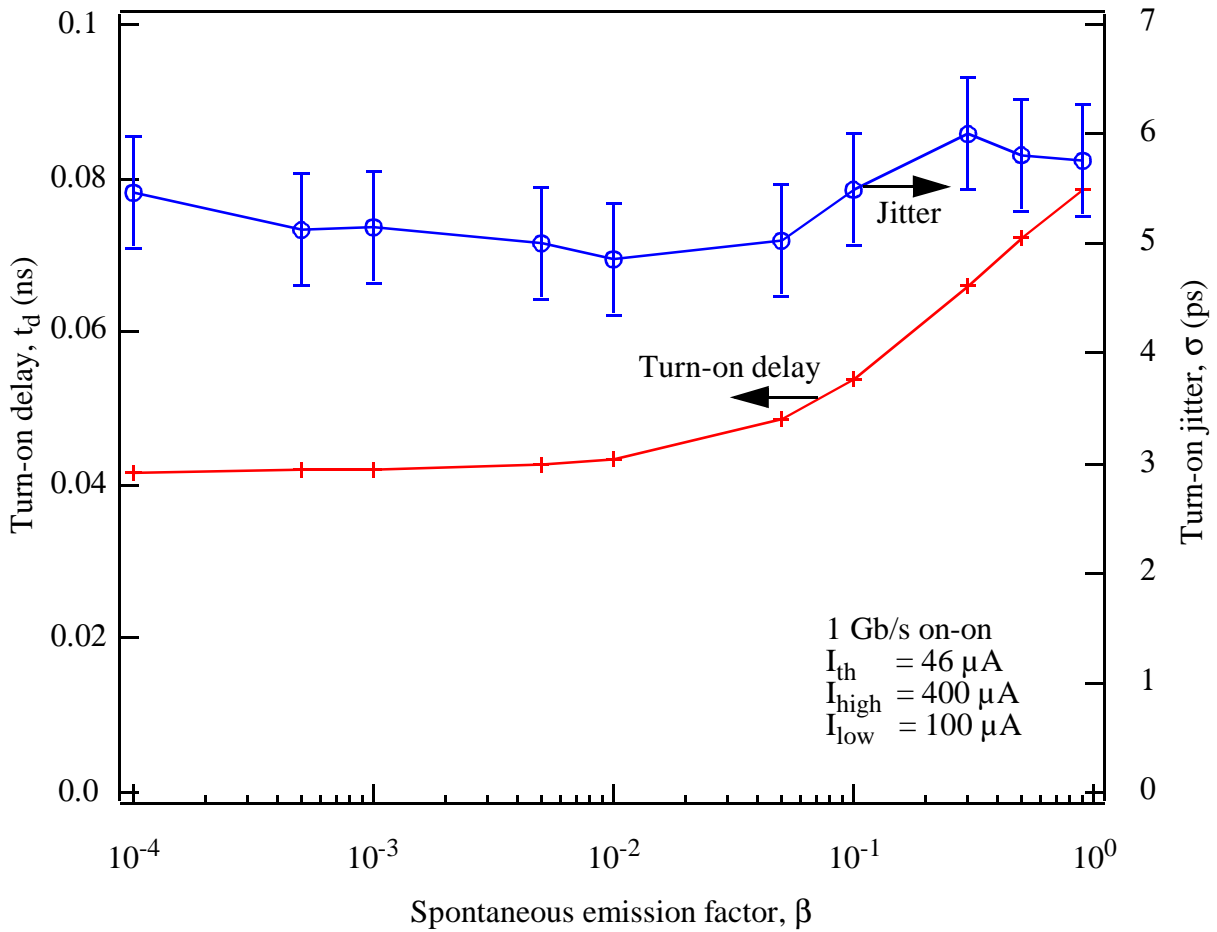


**Figure 2**